PROCEEDINGS OF SCIENCE

ONLINE ICRC 2021
THE ASTROPARTICLE PHYSICS CONFERENCE
Berlin | Germany
37th International Cosmic Ray Conference
12–23 July 2021

The gamma-ray Moon seen by the Fermi LAT over a full solar cycle

Salvatore De Gaetano[a,b,*], **Nicola Giglietto**[a,b], **Francesco Loparco**[a,b], **Mario Nicola Mazziotta**[a], **on behalf of the Fermi Large Area Telescope Collaboration**

[a] *Istituto Nazionale di Fisica Nucleare, Sezione di Bari,*
via Orabona 4, I-70126 Bari, Italy
[b] *Dipartimento di Fisica "M. Merlin" dell'Università e del Politecnico di Bari,*
via Amendola 173, I-70126 Bari, Italy
E-mail: salvatore.degaetano@ba.infn.it, francesco.loparco@ba.infn.it, mario.nicola.mazziotta@ba.infn.it

The Moon is among the brightest gamma-ray sources in the sky. We have reconstructed its gamma-ray spectrum in the energy range from 30 MeV up to a few GeV using the data collected by the Fermi Large Area Telescope during its first 12.5 years of operation since its launch in 2008, a period covering the duration of a whole solar cycle. We have also studied the evolution of the lunar gamma-ray emission by measuring the spectra in 6 months time intervals. The data show a strong correlation with the solar activity. Gamma rays produced on the lunar surface are in fact originated in the interactions of cosmic rays (mainly proton and helium), whose fluxes are affected by solar modulation. We have also developed a model based on the FLUKA simulation code to evaluate the yields of photons produced by cosmic-ray protons and helium nuclei impinging on the Moon. We have then folded the gamma-ray yields obtained from the model with the primary proton and helium spectra measured by the AMS02 and PAMELA experiments in different time intervals and we have compared the simulation results with the experimental data, showing that the simulation reproduces correctly the time evolution of the lunar gamma-ray flux.

37th International Cosmic Ray Conference (ICRC 2021)
July 12th – 23rd, 2021
Online – Berlin, Germany

*Presenter

PoS(ICRC2021)607

1. Introduction

High-energy gamma rays emitted from the Moon are produced in inelastic collisions of cosmic-ray nuclei (CRs) with the lunar surface [1]. The major contribution to the gamma-ray emission comes from the production and subsequent decay of neutral pions in hadronic interactions. The gamma-ray flux from the Moon will be therefore sensitive to the primary CR energy spectra, to the composition of the lunar surface and to the mechanisms of hadronic interactions of CR nuclei with the lunar surface. In this work we have reconstructed the gamma-ray flux from the Moon using the data collected by the Large Area Telescope onboard the Fermi satellite [2] in its first 12.5 years of operation. The analysis procedure is the same as in Ref. [3], with an update in the calculation of the Moon position.

2. Data selection and analysis

The analysis has been performed using a sample of the newest version (P305) of Pass 8 LAT data collected from August 2008 to December 2020 and selecting P8_SOURCE photon events, starting from a minimum energy of 10 MeV. As in Ref. [3], we have defined a signal region and a background region. The signal region is a cone centered on the Moon position, while the background region is a cone centered on a time-offset Moon position of $\Delta t = 14$ days. This choice is due to the fact that the Moon is a moving source, which makes the use of a background template unreliable.

The angular radius of the two regions is given by:

$$\theta = \sqrt{\left[\theta_0 \left(E/E_0\right)^{-\delta}\right]^2 + \theta_{min}^2} \tag{1}$$

with $\theta_{min} = 1°$, $\theta_0 = 5°$, $\delta = 0.8$ and $E_0 = 100$ MeV. This choice reflects the energy dependence of the 68% point spread function (PSF) of the LAT and maximizes the signal-to-noise ratio. The value of θ_{min} accounts for the angular size of the Moon (0.25° angular radius).

The good time intervals (GTIs) for the analysis have been chosen by requiring the following conditions, applied to the Moon or the time-offset-Moon as appropriate:

- LAT taking data in its standard science operation configuration and outside the South Atlantic Anomaly;
- angular separation $< 100°$ between a cone of 15° angular radius centered on the Moon direction and the zenith direction;
- Moon observed with off-axis angle (i.e. angle between the Moon direction and the LAT z-axis) $< 66.4°$;
- Moon at galactic latitudes $|b| > 5°$;
- angular separation $> 20°$ between the Moon and the Sun;
- angular separation $> 20°$ between the Moon and the brightest sources in the 4FGL catalog.

The Moon position is obtained from its ephemeris using a software interfaced to the JPL libraries [4], which provides the Moon right ascension (ra) and declination (dec) with respect to an observer located at the Earth center, and correcting for Fermi orbital parallax. In this work, the Moon apparent coordinates (with respect to the spacecraft) have been obtained from the coordinates of the spacecraft in the GTIs used for the analysis. This method is more precise than the one used in the previous work, in which the parallax correction was implemented by using tabulated values provided in Ref. [5]. This method was validated by performing a cross-check with the `astropy` package [6]. The maximum angular separation between the Moon positions evaluated with the two methods is about 0.01°.

By indicating with $\vec{n}_s = \{n_s(E_1), n_s(E_2), ...n_s(E_n)\}$ and $\vec{n}_b = \{n_b(E_1), n_b(E_2), ...n_b(E_n)\}$ the vectors of the observed signal and background counts in the energy bins used in the analysis, we define the likelihood function:

$$\mathscr{L}(\vec{\phi}_s, \vec{\phi}_b | \vec{n}_s, \vec{n}_b) = \prod_{i=1}^{n} e^{-\mu_s(E_i)} \frac{\mu_s(E_i)^{n_s(Ei)}}{n_s(E_i)!} \prod_{i=1}^{n} e^{-\mu_b(E_i)} \frac{\mu_b(Ei)^{n_b(Ei)}}{n_b(E_i)!} \tag{2}$$

where $\vec{\mu}_s = \{\mu_s(E_1), \mu_s(E_2), ...\mu_s(E_n)\}$ and $\vec{\mu}_b = \{\mu_b(E_1), \mu_b(E_2), ...\mu_b(E_n)\}$ are the vectors of expected counts in the energy bin of signal and background regions. The expected counts, in turn, depend on the signal and background gamma-ray fluxes ϕ_s and ϕ_b:

$$\mu_s(E_i) = \sum_j P_s(E_i|E_j)[\phi_s(E_j) + \phi_b(E_j)] A\, t_s\, \Delta E_j \tag{3}$$

$$\mu_b(E_i) = \sum_j P_b(E_i|E_j)\, \phi_b(E_j)\, A\, t_b\, \Delta E_j \tag{4}$$

where $P_s(E_i|E_j)$ and $P_b(E_i|E_j)$ are the probabilities, respectively in the signal and in the background region, that a photon of energy E_j is observed with energy E_i. These probabilities are computed through Monte Carlo simulations of the LAT, which take into account the instrument pointing history. Here $A = 6\,\mathrm{m}^2$ is the cross sectional area of the spherical surface used for the event generation in the MC simulation and t_s and t_b are the LAT livetimes respectively in the signal and in the background region.

The signal and the background fluxes were reconstructed with a bayesian procedure based on a Monte Carlo Markov Chain (MCMC) implemented in the software toolkit BAT [7]. The starting point for the MCMC is to assume uniform prior probability distribution functions (PDFs) for $\phi_s(E_j)$ and $\phi_b(E_j)$. The posterior PDFs for the two fluxes in each energy bin are then computed by BAT using the likelihood function in Eq. 2. The reconstructed flux in a given energy bin is the one corresponding to the maximum value of its posterior PDF, while the width of the same PDF provides the associated error.

3. Comparison with expected flux

The gamma-ray flux $\phi_\gamma(E_\gamma)$ from the Moon can be evaluated starting from the CR proton and ^{4}He intensities in the solar system, $I_p(T_p)$ and $I_{He}(T_{He})$, T_p and T_{He} being the kinetic energies of proton and Helium respectively, as:

$$\phi_\gamma(E_\gamma) = \frac{\pi R^2}{d^2} \sum_{i=p,He} \int Y(E_\gamma|T_i)\, dT_i = \frac{\pi R^2}{d^2} I_\gamma(E_\gamma) \tag{5}$$

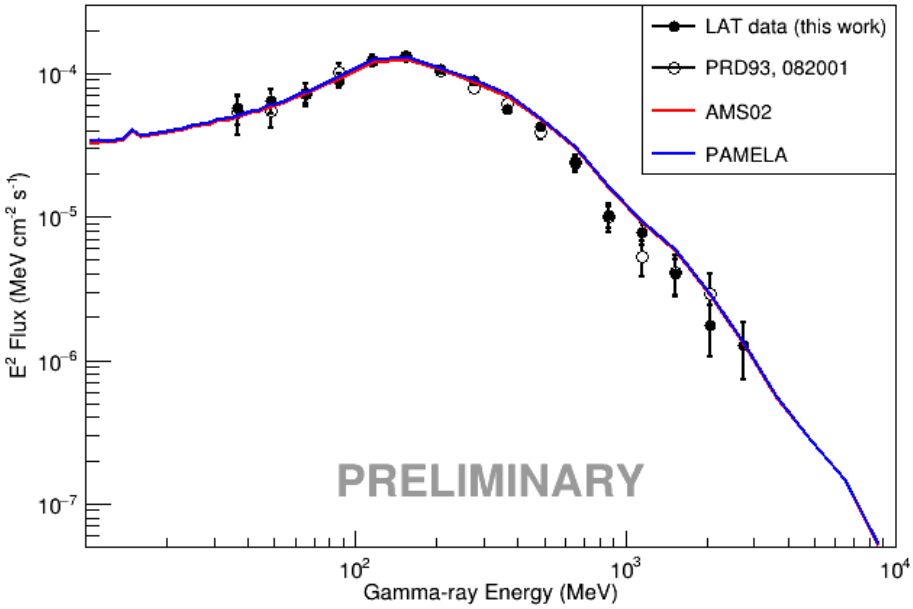

Figure 1: Gamma-ray flux from the Moon in the period from May 2011 to November 2013. The flux reconstructed with the latest version of Pass-8 LAT data (P305) is compared with the flux reconstructed with the previous version of Pass-8 LAT data (P302). The blue and the red curves correspond to the fluxes obtained by folding the gamma-ray yield computed with FLUKA with the proton and He spectra measured by PAMELA and AMS02 in the period from May 2011 to November 2013.

where $Y(E_\gamma|T_i)$ is the gamma-ray yield from the i-th species of CR primaries, d is the LAT-Moon distance and R is the Moon radius.

To evaluate the gamma-ray yield, we implemented a MC simulation of the interactions of CR protons and ^{4}He nuclei with the lunar surface based on the FLUKA code [8]. In our simulation the Moon is described as a sphere of radius $R = 1737.1$ km, consisting of a mixture of different oxides (45% SiO_2, 22% FeO, 11% CaO, 10% Al_2O_3, 9% MgO, 3% TiO_2) with a density $\rho = 1.8\,\mathrm{g/cm^3}$ [9].

The simulation has been validated by comparing the experimental data collected in the period from May 2011 to November 2013 with the predicted gamma-ray flux obtained by folding the gamma-ray yield with the proton and He spectra measured by the AMS02 and PAMELA experiments in the same period [10]. In Fig. 1, the computed gamma-ray spectra are compared with the flux reconstructed using the latest version of the LAT Pass-8 data (P305) and with the flux reconstructed with the previous version of the LAT data (P302). We see that the predictions from the simulation reproduce correctly the data in the whole energy interval.

4. Time evolution studies

We have studied the time evolution of the gamma-ray emission from the Moon dividing the dataset into subsamples, corresponding to periods of 6 months duration. The total time interval exceeds the duration of a full solar cycle. Fig. 2 shows the time evolution of lunar gamma-ray flux above 56 MeV measured by the LAT compared with the predictions obtained from the Monte

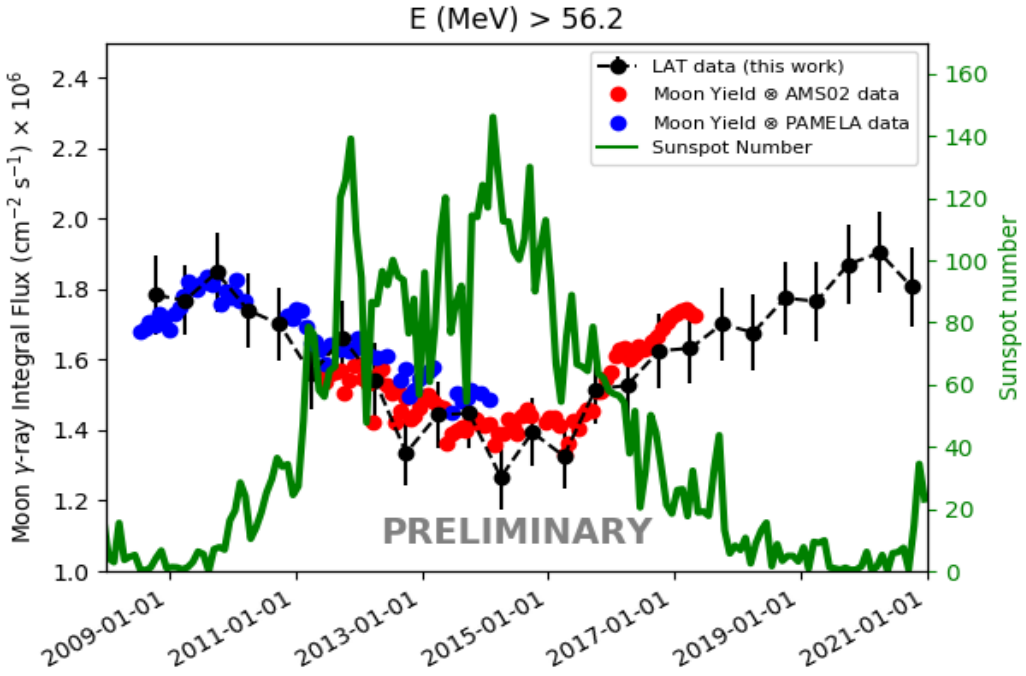

Figure 2: Time evolution of the Moon gamma-ray flux (left y-axis) and of the number of sunspots (right y-axis). Black points indicate the flux measured by the LAT, while blue and red lines correspond to the flux computed by folding the gamma-ray yield obtained with FLUKA with the CR spectra measured by PAMELA and AMS02 respectively.

Carlo simulation described in sec. 3. The plot also shows the time evolution of the number of sunspots, provided by the World Data Center SILSO [11]. We find that the lunar gamma-ray flux is anticorrelated with the solar activity, as already shown in Ref. [3] for a 7-years data sample. This is due to the fact that the intensity of the solar magnetic field increases with the solar activity [12]. Since the flux of charged CRs is modulated by solar magnetic fields and gamma rays are produced by charged CRs impinging on the Moon, the flux of lunar gamma rays at Earth must itself be modulated by solar activity. From Fig. 2 we see that the gamma-ray flux from the Moon has reached a maximum at the end of 2019 and is now starting to decrease, while an increase in the sunspot number is observed, corresponding to the beginning of the 25^{th} Solar Cycle.

5. Conclusions

We reconstructed the gamma-ray spectrum from the Moon by using 12.5 years of Fermi-LAT data, from August 2008 to December 2020. We used the FLUKA code to compute the gamma-ray yield emitted by the Moon due to cosmic rays impinging on it. We folded the yield with the cosmic-ray spectra measured by PAMELA and AMS02 between May 2011 and November 2013. We found that the obtained gamma-ray spectrum reproduces correctly the LAT data in the operational time period of AMS02 and PAMELA. We then performed a time-dependent analysis of the LAT data by dividing the dataset into 6-month-duration subsamples. As expected, we found anticorrelation between the lunar flux and the sunspot number provided by the WDC-SILSO all over the 12.5 years

of data. We also found a maximum in the flux at the end of 2019, corresponding to a minimum in the sunspot number, marking the beginning of the 25^{th} solar cycle.

Acknowledgements

The *Fermi*-LAT Collaboration acknowledges support for LAT development, operation and data analysis from NASA and DOE (United States), CEA/Irfu and IN2P3/CNRS (France), ASI and INFN (Italy), MEXT, KEK, and JAXA (Japan), and the K.A. Wallenberg Foundation, the Swedish Research Council and the National Space Board (Sweden). Science analysis support in the operations phase from INAF (Italy) and CNES (France) is also gratefully acknowledged. This work performed in part under DOE Contract DE-AC02-76SF00515.

References

[1] D. J. Morris, J. Geophys. Res. 89, 10685 (1984)

[2] https://fermi.gsfc.nasa.gov/

[3] M. Ackermann et al., PRD93, 082001 (2016)

[4] https://ipnpr.jpl.nasa.gov/progress_report/42-196/196C.pdf

[5] P. Duffet-Smith and J. Swart, *Practical Astronomy with your Calculator or Spreadsheet*, Cambridge University Press (2011)

[6] https://www.astropy.org/

[7] A. Caldwell, D. Kollar, and K. Krøninger, Comput. Phys. Commun. 180, 2197 (2009)

[8] http://www.fluka.org/

[9] I. V. Moskalenko and T. A. Porter, Astrophys. J. 670, 1467 (2007)

[10] V. Di Felice, C. Pizzolotto et al., PoS(ICRC2017) 1073 (https://pos.sissa.it/301/1073/pdf)

[11] WDC-SILSO, Royal Observatory of Belgium, Brussels

[12] N. Mazziotta el al., *Cosmic-ray interactions with the Sun*, PoS(ICRC2021)